Reprinted from TEXTILE RESEARCH JOURNAL, Vol. 62, No. 12, December 1992
Printed in U. S. A.

Development of a Constitutive Theory for Short Fiber Yarns: Mechanics of Staple Yarn Without Slippage Effect

NING PAN

Division of Textiles and Clothing, University of California, Davis, California 95616, U.S.A.

ABSTRACT

This article reports an attempt to develop a general constitutive theory governing the mechanical behavior of twisted short fiber structures, starting with a high twist case, so that the effect of fiber slippage during yarn extension can be ignored. A differential equation describing the stress transfer mechanism in a staple yarn is proposed by which both the distributions of fiber tension and lateral pressure along a fiber length during yarn extension are derived. Factors such as fiber dimensions and properties and the effect of the discontinuity of fiber length within the structure are all included in the theory. With certain assumptions, the relationship between the mean fiber-volume fraction and the twist level of the yarn is also established. A quantity called the cohesion factor is defined based on yarn twist and fiber properties as well as on the form of fiber arrangement in the yarn to reflect the effectiveness of fiber gripping by the yarn. By considering the yarn structure as transversely isotropic with a variable fiber-volume fraction depending on the level of twist, the tensile and shear moduli as well as the Poisson's ratios of the structures are theoretically determined. All these predicted results have been verified according to the constitutive restraints of the continuum mechanics, and the final results are also illustrated schematically.

Since 1940, there have been extensive developments and improvements in the analysis of yarn mechanical behavior. Research work on yarn mechanics has been reviewed in monographs by Hearle, Grosberg, and Backer [10], Zurek [25], Postle, Carnaby, and De Jong [20] and in an extensive review article by Backer [1]. More specifically, yarn tensile strength and tensile behavior are the properties that have been studied most extensively, and as a result, there is a considerable volume of pertinent literature [4, 8, 13, 19, 22, 23, 24]. However, most of success in this research has been in the area of filament yarns.

Despite wide application of short fiber (staple) yarns, the twist reinforcing or strength generating mechanism as a fundamental structure assembling means for the materials has not been clearly understood. There is no general theory that can be used to explain the mechanics of such structures [6, 21]. The problems in understanding the structural mechanics of staple yarns are primarily caused by two factors as indicated, for example, by Goswami *et al.* [5], that is, the discontinuities in fiber length and the slippage of fibers during yarn extension. Factors such as twist and fiber migration (*i.e.*, variation in radial position in a yarn) in staple yarns acquire different dimensions, since they are the only reasons why a bundle of short fibers is held together in a linear assembly. Moreover, in staple fiber yarns, the fiber-volume fraction is not only low, but also variable, with the result that the structure has no clearly defined surface.

In addition, because of the changing structure of the short fiber yarn at different twist levels, it is essential to consider the yarn fiber-volume fraction, and consequently all the mechanical properties of the yarn, to be variables of yarn twist. This makes the analysis extremely difficult.

Another difficulty in developing a theory for short fiber yarns relates to the statistical nature of the parameters involved. Irregularity and randomness of the structural parameters of the short fiber yarns are their inherent features [17]. In addition, in order to make any progress in predicting the strength of staple yarns, it is important to address the problem of the fracture process and the load sharing mechanism between fibers in a yarn. A thorough study of these issues will permit us to establish the criterion of yarn failure and the strength and fracture behavior of the yarn to be predicted.

As stated in reference 21, "because of the primary function of twist and migration, it is in practice more important to develop a satisfactory theoretical treatment of the mechanics of short fiber yarns. This is particularly desirable if progress is to be made in the engineering design of short fiber yarns in order to make use of the increasing number of available fiber types, the vast number of possible blends, and of new yarn structures which might come from new methods of spinning. If the basic mechanical analysis is solved, the use of computer modeling techniques should enable real practical progress to be made."

There have been several attempts to establish more fundamental theories for short fiber yarns such as the work done by Hearle [10], Zurek [25], and Carnaby [20] using various approaches based on the principle of force-deformation analysis. The complexity of applying a mathematical treatment to staple yarn structure often prevents some of the theoretical models from being useful practical tools for prediction. Also, there have been studies to analyze short fiber yarns by means of the energy approach [10, 20]. This method, however, is unable to deal with the fiber slippage effect because of the energy dissipation involved. The finite element method has also been used to deal with the structure [20]. This approach provides only numerical solutions.

Certainly, a subject of this sort can be approached from several different directions and at various levels. For example, we could gather very extensive data from testing and manipulate them into a form with master curves in terms of nondimensional variables like those used in fluid turbulence analysis and fracture mechanics. Even though such approaches can be useful and convenient, the results are limited to the conditions under which data are obtained. The method has no power to predict behavior outside the range of laboratory experience. Our goal in this study, therefore, is to develop a relatively rigorous theory of the constitutive equation for the staple yarn structure. A carefully derived theory has as its basis certain assumptions or hypotheses that give the boundaries of applicability of the results. Within these boundaries, the theory has a full and complete capability to model actual behavior.

This series of papers consists of several parts that present a general theory of the mechanics of staple fiber yarns. In Part I, we start with a short fiber yarn whose twist level is so high that the interfiber slippage during yarn extension can be ignored. We then propose a theoretical analysis of the distributions of fiber tension and the transverse stresses in a staple yarn, taking account of the effects of definite fiber length. Furthermore, we establish a constitutive relationship for the whole yarn system through which material constants such as yarn tensile and shear moduli as well as yarn Poisson's ratios are calculated based on fiber properties, yarn twist level, and fiber-volume fraction. There are some theoretical verifications of the results as well.

In Part II, we will deal with the problem of fiber slippage during yarn extension. We will develop a modified constitutive relationship taking fiber slippage into account. There will be a detailed parametric study to examine the effects on yarn mechanical behavior of fiber properties and yarn structural parameters.

In the later parts of this series, we will investigate the effect of fiber path in a yarn by proposing several different density functions for the statistical distribution to describe fiber orientations. In addition, a fiber bending mechanism will be included in the analysis. Also we will address the effect of fiber blending on yarn behavior and the problems related to the stochastic nature of yarn fracture and strength due to structural irregularities. The main approach of this series is the theoretical derivations, though experimental results previously available are used wherever possible to verify the theoretical predictions.

Yarns as Transversely Isotropic Structures

Because staple fiber yarn is such a complex structure, certain assumptions have to be made before any theoretical investigation can proceed. The yarn in this study is the so-called idealized staple fiber yarn as defined by Hearle [10]. We will adopt all the assumptions made in reference 10 except that (a) the yarn fiber-volume fraction (yarn packing density or specific volume) is no longer assumed constant, but is allowed to change along with the yarn twist level. (b) Uniformity of both tension and the transverse forces on a fiber in a tensioned yarn is not required. In fact, we will show that both these forces vary along the fiber length due to the definite fiber length (or the discontinuity of fiber length) in the yarn. (c) Shear effects in a yarn are included. Also, we will add one more assumption that was only implied in reference 10: (d) The twist level of the yarn is so high that the drafting force between fibers when twist is zero [7] is negligible.

All real materials, when studied on a sufficiently small scale, display a discrete molecular or atomic structure. However, if one is concerned only with the effects over distances appreciably greater than the distance between these microelements, one can replace the discontinuous microscopic medium with a hypothetical continuum. Naturally the same principle applies, as suggested by Carnaby [20], to fibrous structures. By considering the fibrous structure as a continuum, one can then use the well documented and powerful methods of continuum mechanics to deal with the problems associated with the mechanical behavior of the yarn structure.

We first set a Cartesian coordinate system X_1, X_2, X_3 in a staple yarn structure, where X_3 lies along the yarn axis, and let the angle between the X_3 axis and the axis of an arbitrary fiber within the yarn be θ, and that between the X_1 axis and the normal projection of the fiber axis onto the X_1X_2 plane be ϕ. Then the orientation of any fiber can be defined uniquely by an angle pair (θ, ϕ), provided $0 \le \theta \le \pi$ and $0 \le \phi \le \pi$ as shown in Figure 1.

One of the fundamental tasks in studying the mechanical behavior of a medium is to derive its stress-strain or constitutive relationships. For media of different natures or types, these relationships are very different, as indicated by the theory of continuum mechanics. In the case of the ideal yarn model defined above, the fibers can be assumed to be arranged in the transverse plane in such a manner that there is no preferential packing geometry in the plane, thus making the plane mechanically isotropic. The yarn structure can then be treated as a transversely isotropic material as indicated in reference 20. Consequently, its stress-strain relationships can be expressed by the following equation:

$$\begin{bmatrix} \epsilon_{11} \\ \epsilon_{22} \\ \epsilon_{33} \\ \gamma_{12} \\ \gamma_{23} \\ \gamma_{31} \end{bmatrix} = \begin{bmatrix} \frac{1}{E_T} & -\frac{\nu_{TT}}{E_T} & -\frac{\nu_{LT}}{E_L} & 0 & 0 & 0 \\ -\frac{\nu_{TT}}{E_T} & \frac{1}{E_T} & -\frac{\nu_{LT}}{E_L} & 0 & 0 & 0 \\ -\frac{\nu_{TL}}{E_T} & -\frac{\nu_{TL}}{E_T} & \frac{1}{E_L} & 0 & 0 & 0 \\ 0 & 0 & 0 & \frac{1}{G_{TT}} & 0 & 0 \\ 0 & 0 & 0 & 0 & \frac{1}{G_{TL}} & 0 \\ 0 & 0 & 0 & 0 & 0 & \frac{1}{G_{TL}} \end{bmatrix} \times \begin{bmatrix} \sigma_{11} \\ \sigma_{22} \\ \sigma_{33} \\ \tau_{12} \\ \tau_{23} \\ \tau_{31} \end{bmatrix} , \quad (1)$$

where 1, 2, and 3 refer to the X_1, X_2, X_3 directions in the Cartesian coordinate system, and E_L is the longitudinal modulus governing uniaxial loading in the longitudinal (X_3) direction, ν_{LT} is the associated Poisson's ratio governing induced transverse strains, E_T is the transverse modulus governing uniaxial loading in the transverse (X_1 or X_2) direction, ν_{TL} is the associated Poisson's ratio governing induced longitudinal strains, ν_{TT} is the associated Poisson's ratio governing resultant strains in the remaining orthogonal transverse (X_1 or X_2) direction, G_{TL} is the longitudinal shear modulus governing shear in the longitudinal direction, and G_{TT} is the transverse shear modulus governing shear in the transverse plane. A comprehensive description of the mechanical behavior of a staple yarn relies on the determination of these material constants.

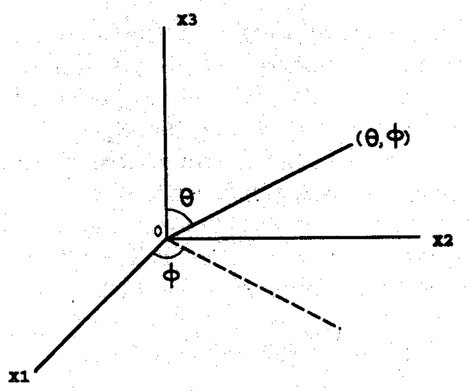

FIGURE 1. The Cartesian coordinate system and a fiber in the yarn.

Also, in the case of transverse isotropy, there are the following interrelationships or restrictions on the range of permitted values for these material constants [2]:

$$E_L, E_T, G_{TL}, G_{TT} > 0 \quad , \quad (2)$$

$$G_{TT} = \frac{E_T}{2(1 + \nu_{TT})} \quad , \quad (3)$$

$$\frac{\nu_{TL}}{E_T} = \frac{\nu_{LT}}{E_L} \quad , \quad (4)$$

$$|\nu_{TL}| \le \left(\frac{E_T}{E_L}\right)^{1/2} \quad , \quad (5)$$

$$|\nu_{LT}| \le \left(\frac{E_L}{E_T}\right)^{1/2} \quad . \quad (6)$$

These restrictions will be used to verify the theoretical results derived in this study.

A staple yarn is made of short fibers twisted with varying orientations within the structure. Since it is impractical to deal with fibers of different orientations individually, a statistical approach, as used in references 15 and 16, is usually a better, or the only, alternative.

To do this, a known form of the function to describe fiber orientation probability density is required.

Let the probability of finding the orientation of a fiber in the infinitesimal range of angles $\theta \sim \theta + d\theta$ and $\phi \sim \phi + d\phi$ be $\Omega(\theta, \phi) \sin \theta d\theta d\phi$, where $\Omega(\theta, \phi)$ is the still unknown density function of fiber orientation and $\sin \theta$ is the Jacobian of the vector of the direction cosines corresponding to θ and ϕ. The following normalization condition must be satisfied:

$$\int_0^q d\theta \int_0^\pi d\phi \Omega(\theta, \phi) \sin \theta = 1 \quad , \tag{7}$$

where q is the upper limit of the polar angle θ.

Stresses on an Arbitrary Fiber in a Short Fiber Yarn

Because of the inherent fiber length discontinuities in a staple yarn, when the yarn is under tension, the resulting tensile stress on each individual fiber cannot be a constant along its length, as assumed in the continuous filament yarn case. As described qualitatively by Hearle [10], the stress will be zero at both ends of a fiber, because no force can be applied to the tips of the fiber. It will then rise gradually to the maximum value determined by the yarn extension due to the transverse forces generated in the yarn, which grips the fiber through the neighboring fibers by means of the frictional interactions. A theoretical description of the distribution of fiber stresses is thus desirable in order to reveal the effect of these length discontinuities and to deal with the problem of fiber end slippage during yarn tensioning. This section focuses on determining both tensile and transverse stresses on an arbitrary fiber within the yarn.

Tensile Stress Distribution

Based on the similarity of the stress transfer mechanism between the two structures, a staple yarn can be considered analogous to a short fiber composite; a fiber can be viewed as embedded in a matrix made of the neighboring fibers (see Figure 2), except that this fiber adheres to the matrix by means of frictional force rather than chemical bonding as in a composite. To begin with, let us assume that the twist level of the yarn is so high that there is no slippage between fibers during yarn extension.

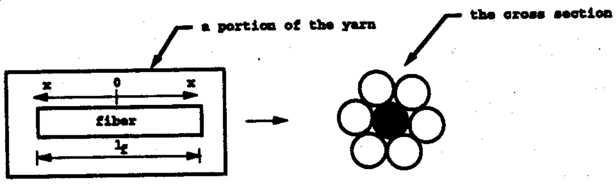

FIGURE 2. A fiber embedded in the matrix made of adjacent fibers in a yarn.

Assume that the yarn consists of short fibers, each of constant length l_f and of a circular cross section of radius r_f. Also suppose the yarn as a whole is subject to a strain ϵ_y, which will cause a strain ϵ_f in an arbitrary fiber. Let x and y locate at and represent the fiber axial direction and the yarn axial direction. If C_{px} is the axial load in the fiber at a distance x from the fiber center, then similar to the treatment of Cox [3], we have

$$\frac{dC_{px}}{dx} = H(u_f - v_y) \quad , \tag{8}$$

where u_f is the longitudinal displacement in the fiber and v_y is the component in the fiber direction of the corresponding displacement the yarn would undergo at the same point if the fiber were absent. H is a constant, the value of which depends on the geometrical arrangement of the fibers and the yarn mechanical properties. Also

$$C_{px} = E_f A_f \frac{du_f}{dx} \quad , \tag{9}$$

where E_f and A_f represent the tensile modulus and the cross-sectional area of the fiber. Differentiating Equation 8 and substituting 9, we get

$$\frac{d^2C_{px}}{dx^2} = H\left(\frac{du_f}{dx} - \frac{dv_y}{dx}\right) = H\left(\frac{C_{px}}{E_f A_f} - \frac{dv_y}{dx}\right) \quad . \tag{10}$$

Now $\frac{dv_y}{dx}$ is, in fact, the component of the yarn strain in the direction of the fiber axis, or in other words, the fiber strain ϵ_f caused by the yarn strain ϵ_y, *i.e.*,

$$\frac{dv_y}{dx} = \epsilon_f \quad . \tag{11}$$

The value of ϵ_f is to be determined based on the fiber path in the yarn. Inserting this relation into Equation 10 yields

$$\frac{d^2C_{px}}{dx^2} = H\left(\frac{C_{px}}{E_f A_f} - \epsilon_f\right) \quad . \tag{12}$$

The solution of this differential equation has been given [3] as

$$\sigma_f = \frac{C_{px}}{A_f} = E_f \epsilon_f \left[1 - \frac{\cosh(nx/r_f)}{\cosh(ns)}\right] \quad , \tag{13}$$

where

$$n = \frac{l_f}{2s}\sqrt{\frac{H}{E_f A_f}} \qquad (14)$$

is a factor dependent on H and

$$s = \frac{l_f}{2r_f} \qquad (15)$$

is the so-called fiber aspect ratio.

Equation 13 gives the fiber tensile stress distribution in terms of fiber properties, yarn properties, and fiber strain, provided we can determine the constant n. In fact, n or H can be derived using a treatment similar to the one Cox proposed [3].

Let us consider again the arbitrary fiber within the yarn and the surrounding circumferential layer of the matrix made of adjacent fibers as shown in Figure 2. Assume all fibers are arranged in the yarn regularly without folds or kinks, so the distance between the center of this fiber and the centers of other fibers in the layer is $2r_f$. If $\tau(r)$ is the shear stress in the direction of the fiber axis on planes parallel to this axis, where r is the radial position in the yarn, then at the surface of the fiber $r = r_f$, we have

$$\frac{dC_{px}}{dx} = -2\pi r_f \tau(r_f) = H(u_f - v_y) \quad . \qquad (16)$$

Therefore,

$$H = -\frac{2\pi r_f \tau(r_f)}{(u_f - v_y)} \quad . \qquad (17)$$

Now let w be the actual displacement in the yarn close to the fiber and assume that there is no slippage between the fiber and the matrix. Then at the surface of the fiber, we have $w = u_f$, and at a distance from the fiber axis equal to $2r_f$, $w = v_y$. If we consider the moment equilibrium of the portion between r_f and $2r_f$, we have

$$2\pi r \tau(r) = \text{constant} = 2\pi r_f \tau(r_f) \quad , \qquad (18)$$

and so the shear strain in the yarn is given by

$$\frac{dw}{dr} = \frac{\tau(r)}{G_{TL}} = \frac{r_f \tau(r_f)}{r G_{TL}} \quad , \qquad (19)$$

where G_{TL} is the mean longitudinal shear modulus of the yarn whose value or expression is to be determined. Here we have assumed an elastic shear behavior of the yarn.

Integrating from r_f to $2r_f$ and noting that the mean shear modulus G_{TL} is independent of the radial position within the yarn, we have

$$\Delta w = \int_{r_f}^{2r_f} dw = \frac{r_f \tau(r_f)}{G_{TL}} \ln(2r_f/r_f) = \frac{r_f \tau(r_f)}{G_{TL}} \ln 2 \quad . \qquad (20)$$

As $\Delta w = (v_y - u_f)$, using Equations 17 and 20 yields

$$H = \frac{2\pi G_{TL}}{\ln 2} \quad . \qquad (21)$$

Then we get the expression for n as

$$n = \frac{l_f}{2s}\sqrt{\frac{H}{E_f A_f}} = \frac{l_f}{2s}\sqrt{\frac{G_{TL}}{E_f}\frac{2\pi}{A_f \ln 2}} = \sqrt{\frac{G_{TL}}{E_f}\frac{2}{\ln 2}} \quad . \qquad (22)$$

In fact, n is an indicator of the gripping effect of the yarn structure on each individual fiber. We therefore name it the cohesion factor, which is obviously a very important system property, and depends on the ratio of yarn shear modulus G_{TL} and fiber tensile modulus E_f as well as the fiber arrangement within the yarn reflected in the analysis above.

DISTRIBUTION OF TRANSVERSE STRESS

Shear stress $\tau(r)$, on the other hand, acts in the form of a frictional stress and is related to the transverse pressure g_r by

$$\tau(r) = \mu g_r \quad . \qquad (23)$$

For simplicity, we have adopted Amonton's friction law here, although it could, of course, be replaced by more sophisticated theories. This frictional stress is the sole cause of stress transference between the yarn and its constituent fibers. Because

$$\pi r_f^2 \sigma_f = -2\pi r_f \mu g_r \quad , \qquad (24)$$

we therefore have

$$g_r = -\frac{r_f}{2\mu}\frac{d\sigma_f}{dx} = \frac{n}{2\mu} E_f \epsilon_f \frac{\sinh(nx/r_f)}{\cosh(ns)} \quad . \qquad (25)$$

This gives the distribution of the transverse stress on the fiber.

The equations above show that the stresses along the fiber length are by no means constant, due to the limited fiber length. Instead, fiber tension is zero at the fiber ends and then ascends toward the fiber center. Also, the transverse stress varies accordingly because of the interrelations between the two. In other words, the stress fields within the staple yarn are not continuous, owing to the discontinuity of the fiber length.

In this analysis, the effect of stress transfer across the fiber ends is neglected, which will cause an extra load on both the fiber and the fiber matrix in this region. However, this effect is considered insignificant [18] as long as the fiber aspect ratio $s > 10$. Also, the influence of stress concentration across the fiber ends, which will lead to greater shear stress [12] and will affect the slip behavior of the fiber ends, is ignored.

Average Stress on an Arbitrary Fiber

The average tensile stress over the definite fiber length can be calculated from Equation 13 by integrating over the fiber length to give

$$\bar{\sigma}_{fl} = E_f \epsilon_f \left[1 - \frac{\tanh(ns)}{ns} \right] = E_f \eta_l \epsilon_f \quad , \qquad (26)$$

where

$$\eta_l = 1 - \frac{\tanh(ns)}{ns} \qquad (27)$$

is called the length efficiency factor. When fiber length or $s \rightarrow \infty$, then $\eta_l = 1$.

Maximum Values and Ratio of Tensile and Shear Stresses

Note from Equation 13 that $\sigma_f = 0$ at both ends where $x = l_f/2$. The maximum stress occurs at the center position $x = 0$, and then

$$\sigma_{\max} = E_f \epsilon_f \left[1 - \frac{1}{\cosh(ns)} \right] \quad . \qquad (28)$$

The maximum value of g_r occurs at the fiber ends, *i.e.*, $x = l_f/2$,

$$g_{\max} = \frac{n}{2\mu} E_f \epsilon_f \tanh(ns) \quad , \qquad (29)$$

and g_r is zero at the middle of the fiber.

The ratio of the maximum value of shear stress to the maximum tensile stress in the fiber is

$$\frac{g_{\max}}{\sigma_{\max}} = \frac{n}{2\mu} \coth(ns/2) \quad . \qquad (30)$$

This ratio is important because it is a reflection of the intrinsic properties of the fibers and the yarn, and is independent of yarn strain.

The preceding equations provide distributions of all internal stresses along a fiber length. Specific examples and illustrations will be given in the discussion section of this paper. If the fiber-yarn strain relationship is known, these equations also predict the stress distribution radially across the yarn.

Determining Fiber-Volume Fraction

It is well known that the yarn fiber-volume fraction V_f is a key parameter that will affect all the other yarn properties. It is also true that the yarn fiber-volume fraction is not uniform throughout a yarn cross section. Therefore, in this study, we have used the mean fiber-volume fraction V_f averaged over the whole yarn cross section. But even this mean fiber-volume fraction, for a given fiber amount, depends on yarn extension and twist level. An iterative expression for the fiber-volume fraction in terms of the yarn extension will be provided in another paper in this series. The establishment of an analytical expression for V_f, which includes the effect of yarn twist level, is an important task in this study.

It is possible to develop a very rigorous expression to specify such a relationship based on geometric and mechanical analysis. Some of our early attempts, however, showed that such an expression is most likely to be very complex and impractical. Instead, we have used a partially empirical approach here to provide a much simpler and still quite reasonable result.

The relationship between V_f and the yarn twist level T_y has been studied experimentally [9], and the result implies the following relationship:

$$\frac{dV_f}{dT_y} = A - BV_f \quad , \qquad (31)$$

where A and B are constants. That is, the change rate of V_f versus the yarn twist factor T_y possesses a maximum when V_f is at its lowest value V_{f0}, decreases as V_f is increasing, and becomes zero when V_f reaches its highest level V_{fm}.

The solution for this equation is

$$V_f = V_{fm} - V_{fm} e^{-BT_y} + V_{f0} e^{-BT_y} \quad . \qquad (32)$$

By properly choosing a factor m, V_{f0} can always be expressed in terms of V_{fm}, *i.e.*,

$$V_{f0} = mV_{fm} \quad . \qquad (33)$$

So finally we have

$$V_f = V_{fm}(1 - (1 - m)e^{-BT_y}) \quad . \qquad (34)$$

From the experimental evidence [9], we find $V_{fm} = 0.7$, $V_{f0} = 0.154$, and $B = 0.195$. The equation above becomes

$$V_f = 0.7(1 - 0.78e^{-0.195T_y}) \quad . \qquad (35)$$

Figure 3 shows the result using this equation. In this study, we will use this equation to calculate other parameters. Obviously all its factors can be modified to suit other particular yarns.

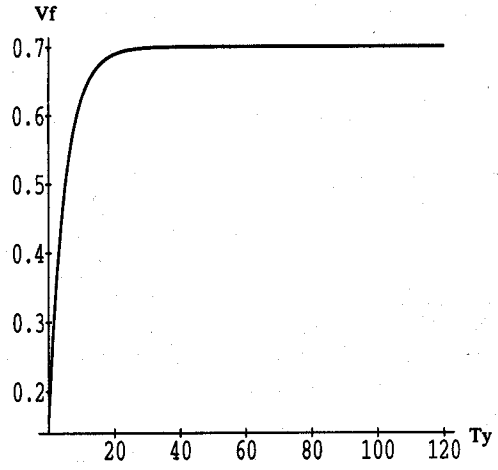

FIGURE 3. The assumed result of the fiber-volume fraction V_f versus yarn twist T_y.

Loads and Deformations on an Arbitrary Fiber Within the Yarn

The load applied to the yarn must be transferred to each individual fiber through fiber contacts by means of the friction mechanism. Therefore, the forces on each fiber are most likely distributed in a discrete fashion along its length. For simplicity, however, in our analysis we will replace it by a concentrated load averaged over all the distributed loads on a fiber. Also, we will take the whole fiber as the unit for deformation analysis, as we did in the preceding section dealing with fiber stress distribution. Let us name the concentrated load on each fiber C_j and assume that it is acted on both ends of the fiber in the direction j as a result of the external load P_j on the yarn. This load C_j can be further resolved into components C_{jp} acting in the axial direction of the fiber and C_{jn} normal to the fiber axis, as shown in Figure 4.

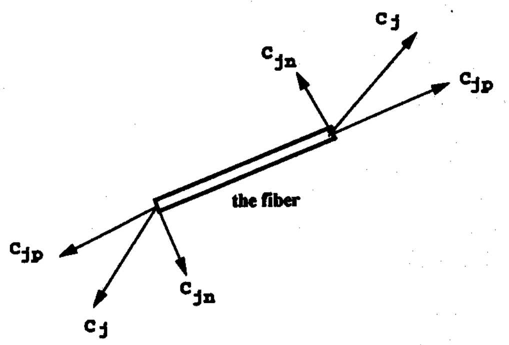

FIGURE 4. The forces and their components on a fiber.

The component C_{jp} will cause axial elongation on the fiber, while the component C_{jn} will result in bending deformation. The bending problem in a general fibrous assembly has been analyzed by Lee and Lee [15], and their results can be helpful to cases where the bending effect is important. Since fiber tensile breakage is the dominate form of fiber failure in a yarn, the bending effect is therefore considered less significant. Meanwhile, including bending deformation in the analysis will greatly increase the complexity of the final results. Therefore, to start with, we will focus only on axial deformation.

According to Lee's analysis [14], the expressions of the projections of C_{jp} ($j = 1, 2, 3$) onto the Cartesian coordinate system in terms of the fiber orientation are

$$C_{1p} = C_1 \sin\theta \cos\phi(\sin\theta\cos\phi\vec{i}_1 + \sin\theta\sin\phi\vec{i}_2 + \cos\theta\vec{i}_3) \quad , \quad (36)$$

$$C_{2p} = C_2 \sin\theta \sin\phi(\sin\theta\cos\phi\vec{i}_1 + \sin\theta\sin\phi\vec{i}_2 + \cos\theta\vec{i}_3) \quad , \quad (37)$$

$$C_{3p} = C_3 \cos\theta(\sin\theta\cos\phi\vec{i}_1 + \sin\theta\sin\phi\vec{i}_2 + \cos\theta\vec{i}_3) \quad . \quad (38)$$

The axial deformation δ_{aj} on the fiber caused by C_{jp} can be found using Equation 26. Since we have

$$\delta_{aj} = l_f\epsilon_f = l_f\frac{\bar{\sigma}_{fl}}{E_f\eta_l} \qquad (39)$$

and

$$\bar{\sigma}_{fl} = \frac{C_{jp}}{A_f} \quad , \qquad (40)$$

combining the two gives

$$\delta_{aj} = \frac{C_{jp}l_f}{A_fE_f\eta_l} \quad . \qquad (41)$$

Note that the load and hence the deformation have three components, as indicated in Equations 36–38. For the same external load, their values will be different for fibers with different orientations θ and ϕ.

Deformations, Strains, and Stresses of a Representative Yarn Element

In the preceding sections, we have derived all the stresses, loads, and deformations for an arbitrary fiber. By using a proper approach, we will be able to extend our analysis from a single fiber to the whole yarn so as to study yarn behavior.

Figures 2 and 5 show the arbitrary fiber with its surrounding matrix made of neighboring fibers. Since this portion is taken arbitrarily from the yarn, it is considered a representative element of the yarn. The dimensions of this yarn element can be defined as follows: First, the projected lengths of the arbitrary fiber onto the three coordinate axes are

$$l_{f1} = l_f \sin\theta \cos\phi \quad , \qquad (42)$$

$$l_{f2} = l_f \sin\theta \sin\phi \quad , \qquad (43)$$

and

$$l_{f3} = l_f \cos\theta \quad . \qquad (44)$$

The statistical average dimensions of this yarn element can then be determined by integrating these projections of the arbitrary fiber, using the density distribution function, over all the possible fiber orientation ranges as

$$\bar{l}_{fj} = l_f K_j \quad , \qquad (45)$$

where the orientational factors K_j were derived by Lee and Lee [15]:

$$K_1 = \int_0^\pi d\theta \int_0^\pi d\phi \sin^2\theta \cos\phi\,\Omega(\theta, \phi) \quad , \qquad (46)$$

$$K_2 = \int_0^\pi d\theta \int_0^\pi d\phi \sin^2\theta \sin\phi\,\Omega(\theta, \phi) \quad , \qquad (47)$$

$$K_3 = \int_0^\pi d\theta \int_0^\pi d\phi \sin\theta \cos\theta\,\Omega(\theta, \phi) \quad . \qquad (48)$$

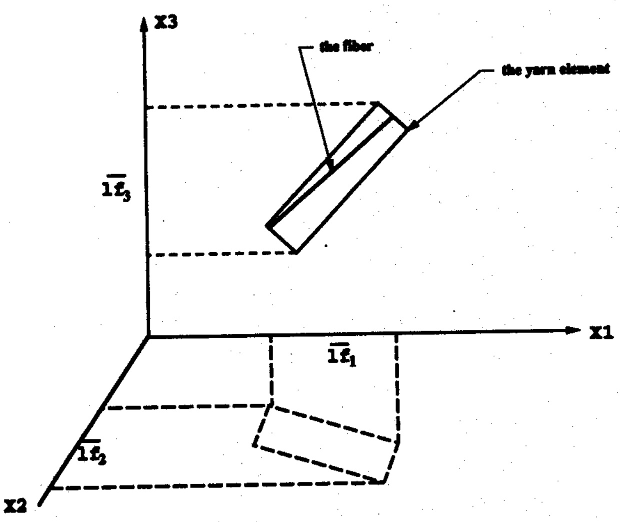

FIGURE 5. A representative element of the yarn and its projected dimensions.

Similarly, the statistical averages of the deformations of this yarn element can also be derived based on the fiber deformations as

$$\bar{\delta}_{jk} = \int_0^\pi d\theta \int_0^\pi d\phi\,\delta_{aj}\Omega(\theta, \phi) = \bar{\delta}_{aj} M_{jk}{}^a \quad , \qquad (49)$$

where

$$\bar{\delta}_{aj} = \frac{C_j l_f}{A_f E_f \eta_l} \qquad (50)$$

is the magnitude of the axial deformations of the yarn element, and $M_{jk}{}^a$ are the respective coefficients representing the effects of fiber orientation and loading direction.

$M_{jk}{}^a$ can be calculated based on Equations 36–38, 41, and 49 as

$$M_{11}{}^a = \int_0^\pi d\theta \int_0^\pi d\phi \sin^3\theta \cos^2\phi\,\Omega(\theta, \phi) \quad , \qquad (51)$$

$$M_{22}{}^a = \int_0^\pi d\theta \int_0^\pi d\phi \sin^3\theta \sin^2\phi\,\Omega(\theta, \phi) \quad , \qquad (52)$$

$$M_{33}{}^a = \int_0^\pi d\theta \int_0^\pi d\phi \cos^2\theta \sin\theta\,\Omega(\theta, \phi) \quad , \qquad (53)$$

$$M_{12}{}^a = M_{21}{}^a = \int_0^\pi d\theta \int_0^\pi d\phi \sin^3\theta \cos\phi \sin\phi\,\Omega(\theta, \phi) \quad , \qquad (54)$$

$$M_{13}{}^a = M_{31}{}^a = \int_0^\pi d\theta \int_0^\pi d\phi \sin^2\theta \cos\theta \cos\phi\,\Omega(\theta, \phi) \quad , \qquad (55)$$

$$M_{23}{}^a = M_{32}{}^a = \int_0^\pi d\theta \int_0^\pi d\phi \sin^2\theta \cos\theta \sin\phi\,\Omega(\theta, \phi) \quad . \qquad (56)$$

In order to determine the strains and stresses on this yarn representative element, we need to know the external load on the element. Because of the axial symmetry of the yarn structure, it is reasonable to assume that all the loads C_j exerted on individual fibers have the same magnitude in the identical direction of the external load P_j. Therefore, we have

$$C_j = \frac{P_j}{N_{fj}} = \frac{P_j A_f}{K_j V_f A_{yj}} \quad , \qquad (57)$$

where A_{yj} is the projected area of the yarn element in direction j and

$$N_{fj} = \frac{K_j V_f A_{yj}}{A_f} \qquad (58)$$

is the projected number of fibers in the same direction.

So the external load can be expressed as

$$P_j = C_j N_{fj} = \frac{C_j K_j V_f A_{yj}}{A_f} \quad . \tag{59}$$

The normal stress on the yarn element due to P_j can thus be defined as

$$\sigma_{jj} = \frac{P_j}{A_{yj}} = \frac{K_j V_f C_j}{A_f} \quad . \tag{60}$$

As in the shear case, we assume that there are two surface tractions P_j and P_k applied as shown in Figure 6 onto the yarn element. Similar to P_j, P_k can be written as

$$P_k = \frac{C_k K_k V_f A_{yk}}{A_f} \quad . \tag{61}$$

For shear force equilibrium, there has to be

$$P_k = P_j \quad . \tag{62}$$

Therefore we have

$$C_k K_k A_{yk} = C_j K_j A_{yj} \quad . \tag{63}$$

For simplicity, without losing generality, we can always select the yarn element in such a way that

$$A_{yk} = A_{yj} \quad . \tag{64}$$

So we get the relationship

$$C_k K_k = C_j K_j \quad . \tag{65}$$

The shear stress is then defined as

$$\tau_{jk} = \frac{P_k}{A_{yj}} = \frac{K_k V_f C_k}{A_f} = \tau_{kj} = \frac{K_j V_f C_j}{A_f} \quad . \tag{66}$$

The strains of this yarn element are derived based on its deformations. The value $\bar{\delta}_{jk}$ shown in Equation 49 is actually the overall deformation of the yarn element in the direction k due to the external load P_j. Therefore the normal strain of the element can be defined as

$$\epsilon_{jj} = \frac{\bar{\delta}_{jj}}{\bar{l}_{fj}} = \frac{\bar{\delta}_{jj}}{l_f K_j} \quad , \tag{67}$$

and the shear strain of such a system can be defined according to Pan and Carnaby [16] as

$$\gamma_{jk} = \frac{\bar{\delta}_{jj} + \bar{\delta}_{kj}}{\bar{l}_{fk}} + \frac{\bar{\delta}_{kk} + \bar{\delta}_{jk}}{\bar{l}_{fj}} \quad . \tag{68}$$

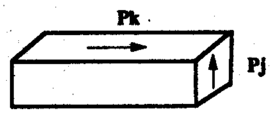

FIGURE 6. The surface tractions on the yarn element.

Determining Yarn Material Constants

Since the yarn element is an arbitrary part or the representative of the yarn, the yarn thus experiences the same stresses and strains as defined in the last section. Consequently, we can calculate the elastic moduli of the yarn as

$$E_{jj} = \frac{\sigma_{jj}}{\epsilon_{jj}} \quad (j = 1, 2 \text{ and } 3) \quad , \tag{69}$$

and its Poisson's ratios as

$$\nu_{jk} = -\frac{\epsilon_{jk}}{\epsilon_{jj}} = -\frac{\dfrac{\bar{\delta}_{jk}}{\bar{l}_{fk}}}{\dfrac{\bar{\delta}_{jj}}{\bar{l}_{fj}}} = -\frac{\bar{\delta}_{jk}\bar{l}_{fj}}{\bar{\delta}_{jj}\bar{l}_{fk}} \quad (j \neq k \text{ and } j, k = 1, 2, 3) \quad , \tag{70}$$

as well as the shear moduli,

$$G_{jk} = \frac{\tau_{jk}}{\gamma_{jk}} \quad (j, k = 1, 2 \text{ and } 3) \quad . \tag{71}$$

If we bring the expressions of σ_{jj} and ϵ_{jj} and the result in Equation 49 into Equation 69 and use the symbols defined in Equation 1 for a transversely isotropic material, with necessary algebraic manipulations the tensile moduli of the yarn become

$$E_L = E_{33} = \frac{V_f E_f \eta_l K_L^2}{M_{LL}^a} \tag{72}$$

and

$$E_T = E_{22} = E_{11} = \frac{V_f E_f \eta_l K_T^2}{M_{TT}^a} \quad , \tag{73}$$

and the Poisson's ratios become

$$\nu_{TL} = \nu_{13} = \nu_{23} = \frac{M_{TL}^a K_T}{M_{TT}^a K_L} \quad , \tag{74}$$

$$\nu_{LT} = \nu_{31} = \nu_{32} = \frac{M_{LT}^a K_L}{M_{LL}^a K_T} \quad , \tag{75}$$

$$\nu_{TT} = \nu_{12} = \nu_{21} = \frac{M_{12}^a K_1}{M_{TT}^a K_2} = \frac{M_{21}^a K_2}{M_{TT}^a K_1} \quad . \tag{76}$$

Note that in Equation 76 the subscripts 1 and 2 are used instead of two Ts, because $M_{TT}^a \neq M_{12}^a$ or M_{21}^a. Since for a transversely isotropic material, $K_1 = K_2 = K_T$, this equation further reduces to

$$\nu_{TT} = \frac{M_{12}^a}{M_{TT}^a} = \frac{M_{21}^a}{M_{TT}^a} \quad . \tag{77}$$

The shear modulus

$$G_{TL} = G_{13} = G_{23} = \frac{E_f V_f \eta_l}{S(T, L)} \quad , \tag{78}$$

where

$$S(T, L) = \frac{(M_{TT}{}^a + M_{LL}{}^a)}{K_T K_L} + \frac{M_{TL}{}^a}{K_T{}^2} + \frac{M_{LT}{}^a}{K_L{}^2} \quad . \tag{79}$$

For the same reason, we distinguish between directions 1 and 2 in the following equation:

$$G_{TT} = G_{12} = G_{21} = \frac{E_f V_f \eta_l}{S(1, 2)} \quad , \tag{80}$$

where

$$S(1, 2) = \frac{2(M_{TT}{}^a + M_{12}{}^a)}{K_T{}^2} \quad . \tag{81}$$

Theoretical Verification of Results

One way to verify these theortically derived results is to check the restrictions given in Equations 2 to 6. First of all, since the orientational factors such as $M_{jk}{}^a$ and K_j always possess positive values, it is obvious that

$$E_L, E_T, G_{TL}, G_{TT} > 0 \quad .$$

Equation 3 requires that

$$G_{TT} = \frac{E_T}{2(1 + \nu_{TT})} \quad .$$

It is easy to show, based on the definitions of E_T and G_{TT}, that

$$\frac{E_T}{G_{TT}} = \frac{2(M_{TT}{}^a + M_{12}{}^a)}{M_{TT}{}^a} = 2\left(1 + \frac{M_{12}{}^a}{M_{TT}{}^a}\right) \quad . \tag{82}$$

According to Equation 77,

$$\frac{M_{12}{}^a}{M_{TT}{}^a} = \nu_{TT} \quad .$$

The condition in Equation 3 is thus satisfied.

The next restraint states that

$$\frac{\nu_{TL}}{E_T} = \frac{\nu_{LT}}{E_L} \quad .$$

This can easily be proved to be true using Equations 72–76, noting that $M_{TL}{}^a = M_{LT}{}^a$. As to the restraints

$$|\nu_{TL}| \leq \left(\frac{E_T}{E_L}\right)^{1/2}$$

and

$$|\nu_{LT}| \leq \left(\frac{E_L}{E_T}\right)^{1/2} \quad ,$$

the specific form of the fiber orientation function is needed in order to evaluate these two conditions.

Yarn Density Function and Fiber Orientation

So far we have derived all the material constants that govern the mechanical behavior of the staple yarns. The only thing remaining to be found is the expression for the distribution density function, which describes the directional orientations of fibers within the yarn. In fact, a successful treatment of fiber orientation and, later on, fiber migration effects relies largely on a satisfactory density function. Unfortunately, determining the density function for a particular case is not always easy. Let us start with the simplest case here, and the more complex ones will be treated in later papers of this series.

For an axially symmetric structure like a yarn, it is easy to see that the azimuthal angle ϕ is uniformly distributed in the range $0 \leq \phi \leq \pi$, so that the density function is independent of ϕ. Moreover, note that the polar angle θ is identical to the helix angle of a fiber in the yarn, and $0 \leq \theta \leq q$, where q is the helix angle of fibers on the yarn surface. The simplest case is to assume that all fibers in a yarn are oriented in a totally random manner within the range q. Because of this randomness of fiber orientation, the density function becomes independent of θ as well. Therefore this density function has the form of

$$\Omega(\theta, \phi) \sin \theta = \Omega_0 \sin \theta \quad , \tag{83}$$

where Ω_0 is a constant whose value is determined using the normalization condition in Equation 7 as

$$\Omega_0 = \frac{1}{\pi(1 - \cos q)} \quad . \tag{84}$$

Using this density function, all the related parameters can be calculated as

$$K_L = \frac{(1 + \cos q)}{2} \quad ,$$

$$K_T = \frac{2(q/2 - 1/4 \sin 2q)}{\pi(1 - \cos q)} \quad ,$$

$$M_{TT}{}^a = \frac{(2/3 - \cos q + 1/3 \cos^3 q)}{2(1 - \cos q)} \quad ,$$

$$M_{12}{}^a = M_{21}{}^a = \frac{(2/3 - \cos q + 1/3 \cos^3 q)}{\pi(1 - \cos q)} \quad ,$$

$$M_{LL}{}^a = \frac{1 + \cos q + \cos^2 q}{3} \quad ,$$

$$M_{LT}{}^a = M_{TL}{}^a = \frac{2 \sin^3 q}{3\pi(1 - \cos q)} \quad .$$

Bringing these results into the relevant equations yields the final results for the longitudinal tensile modulus

$$E_L = \frac{3V_f E_f \eta_l}{4} \frac{(1 + \cos q)^2}{1 + \cos q + \cos^2 q} \quad , \qquad (85)$$

the transverse modulus

$$E_T = \frac{8V_f E_f \eta_l}{\pi^2} \times \frac{(q/2 - 1/4 \sin 2q)^2}{(2/3 - \cos q + 1/3 \cos^3 q)(1 - \cos q)} \quad , \qquad (86)$$

the Poisson's ratios

$$\nu_{LT} = \frac{\sin^5 q}{2(1 - \cos^3 q)(q/2 - 1/4 \sin 2q)} \quad , \qquad (87)$$

$$\nu_{TL} = \frac{16 \sin q(q/2 - 1/4 \sin 2q)}{3\pi^2(2/3 - \cos q + 1/3 \cos^3 q)} \quad , \qquad (88)$$

$$\nu_{TT} = \frac{2}{\pi} \quad , \qquad (89)$$

as well as the shear moduli

$$G_{TT} = \frac{4V_f E_f \eta_l}{\pi(2 + \pi)} \times \frac{(q/2 - 1/4 \sin 2q)^2}{(2/3 - \cos q + 1/3 \cos^3 q)(1 - \cos q)} \quad . \qquad (90)$$

G_{TL} is the same as given in Equation 78 with

$$S(T, L) = \frac{\pi(1 - \cos q) \sin^3 q}{6(q/2 - 1/4 \sin 2q)^2} + \frac{8 \sin^3 q}{3\pi(1 - \cos q)(1 + \cos q)^2} + \frac{\pi(4 - 3 \cos q - \cos^3 q)}{6(q/2 - 1/4 \sin 2q)(1 + \cos q)} \quad . \qquad (91)$$

Calculations and Discussion

The data used for the calculations are listed in Table I. The yarn surface helix angle q is calculated using an equation from Hearle *et al.* [10]. Since they developed this equation based on a continuous filament yarn, which has a more regular structure than a staple yarn, we insert a correction factor a_q into the equation:

$$q = \arctan\left[a_q 10^{-3} T_y \left(\frac{40\pi}{\rho_f V_f}\right)\right] \quad . \qquad (92)$$

In this study, we used $a_q = 2.5$. Because of the correction factor, the upper limit of q will also be slightly higher than what Hearle *et al.* defined for continuous filament yarns [10]. Figure 7 shows the q values corresponding to an increasing yarn twist factor T_y.

TABLE I. The fiber matrix properties used for calculation.

Item	Typical value	Unit
Fiber radius r_f	3×10^{-3}	cm
Fiber length l_f	3.0	cm
Fiber specific density ρ_f	1.31	g/cm³
Fiber modulus E_f	6×10^7	g/cm²
Fiber frictional coefficient μ	0.3	
Fiber aspect ratio $s = \frac{l_f}{2r_f}$	500	

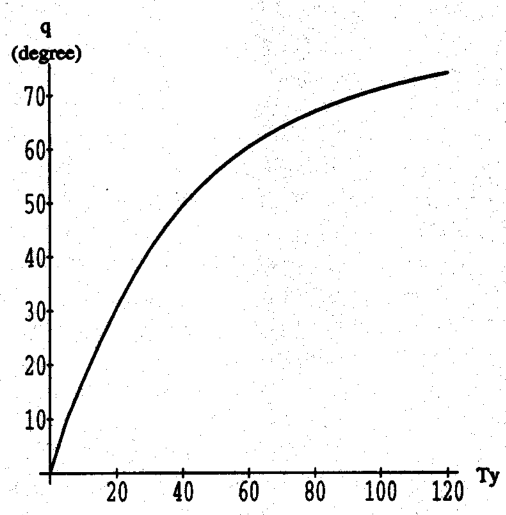

FIGURE 7. The yarn surface helix angle q versus yarn twist T_y.

Since the longitudinal shear modulus G_{TL} in Equation 78 depends on the cohesion factor n, and the latter is in turn determined by the modulus G_{TL} as shown in Equation 22, we used a numerical approach to solve G_{TL} from Equations 78 and 91. We then calculated n and plotted it against the yarn twist factor as shown in Figure 8. By considering the physical meaning of n, we can see from Figure 8 that the gripping force between fibers increases very rapidly with increased yarn twist level, and levels off when twist becomes very high. Note that when we derived n in Equation 22, we assumed that all fibers are packed regularly as shown in

Figure 2. So by applying the corresponding relationships into the integration in Equation 20, it is possible to study the effects on fiber gripping force of irregularities in fiber arrangement such as kinks and reversals.

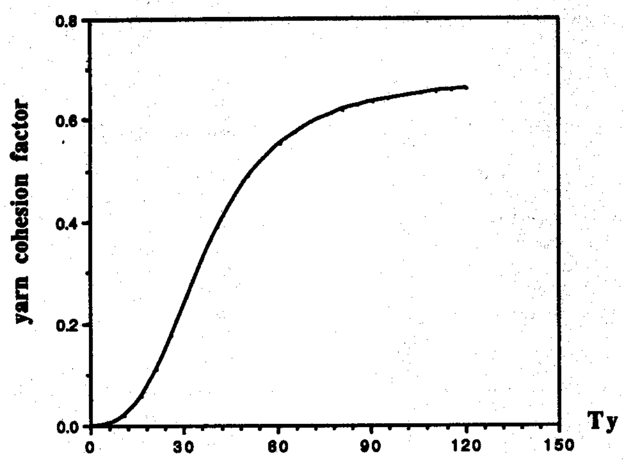

FIGURE 8. The yarn cohesion factor n versus yarn twist T_y.

Also, because all yarn properties are determined by the cohesion factor n or the yarn twist factor T_y, in the following discussion, we will mainly study the relationships between T_y and these yarn properties. Other factors such as fiber properties and orientation, together with the effects of end slippage during yarn extension, will be discussed in subsequent papers.

The shear stress on a fiber in a tensioned yarn is provided in Equations 23 and 25, which clearly give the connection between fiber properties, the yarn cohesion factor, and this stress. For convenience of discussion, we define a dimensionless relative quantity $\tau = \dfrac{\tau(r)}{E_f \epsilon_f}$. Figure 9 shows the results at three different twist levels.

First of all, the distribution of shear stress along a fiber is not constant; it possesses the maximum value at fiber ends, decreases towards the fiber center, and reaches zero at the fiber center. As expected, twist has a profound effect on the shape of the distribution: at a relatively higher twist level, the magnitude of the maximum shear stress at fiber ends not only becomes much greater, it also descends more rapidly to zero within a shorter distance from the fiber ends.

Similarly the relative tensile stress on this arbitrary fiber is $\sigma = \dfrac{\sigma_f}{E_f \epsilon_f}$. As shown by Equation 13, so long

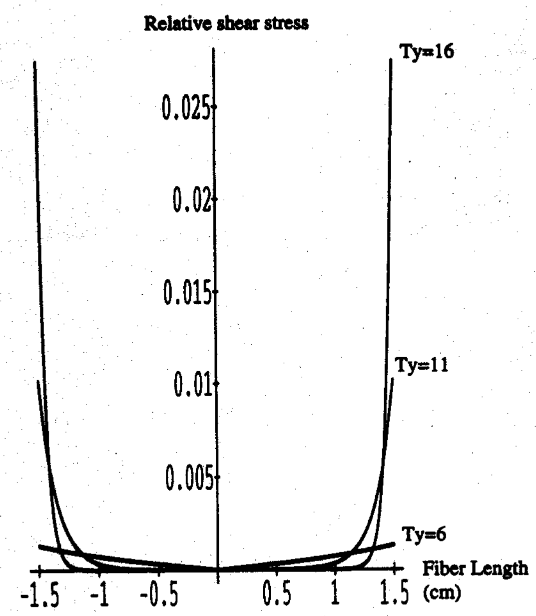

FIGURE 9. The relative shear stress τ on a fiber.

as fibers are not completely slipping, at the region where they are gripped, the distribution of fiber tension is not linear but follows a hyperbolic rule.

The result is given in Figure 10. When the yarn twist level is above a certain value, the fiber tension will build up very quickly from zero at the fiber ends, and reach the value determined by the yarn extension at

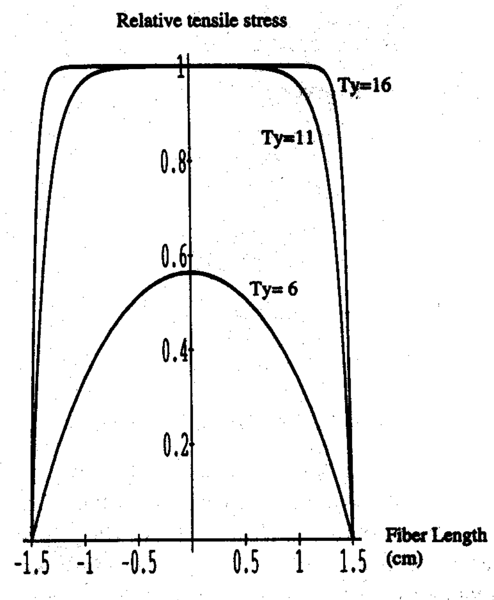

FIGURE 10. The relative tensile stress σ on a fiber.

the middle of the fiber length. However if the twist factor is small, the tension on a fiber will be lower than the value associated with the given yarn extension (at the fiber center, the relative value is less than 1).

Figure 11 gives the ratio of the maximum values of fiber lateral pressure and tensile stress based on Equation 30. This ratio increases as the twist increases, indicating that the maximum value of lateral pressure increases faster than the tension. This ratio can also exceed 1 at extremely high twist.

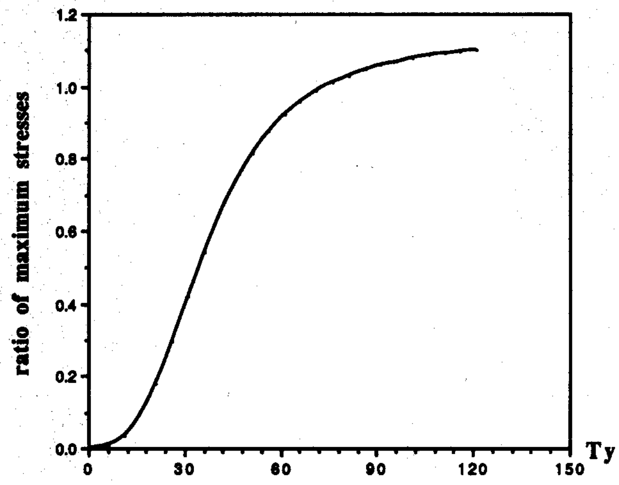

FIGURE 11. Ratio of maximum values of pressure g_{max} and tensile stress σ_{max}.

To study the effect of definite fiber length, we provide in Figure 12 the relation of the so-called fiber length efficiency factor η_l and T_y. From Equations 26 and 27, we can see that

$$\eta_l = \frac{\bar{\sigma}_{fl}}{E_f \epsilon_f} = 1 - \frac{\tanh(ns)}{ns} \quad . \tag{93}$$

That is, this length efficiency factor actually represents the relative average tensile stress on a fiber. Its value is far less than unity when the yarn twist is below a certain level. In other words, a staple yarn becomes equivalent to a filament yarn in terms of the fiber contribution to yarn strength once the twist level gets high enough. Note that η_l is the only factor that reflects the effect of fiber dimensions (by means of the fiber aspect ratio s).

The following figures provide the results of the predicted yarn properties. As indicated in the last section, all yarn moduli are proportional to the fiber tensile modulus E_f. Consequently, the figures of yarn moduli are plotted in terms of the relative scale using the ratio of yarn moduli and E_f.

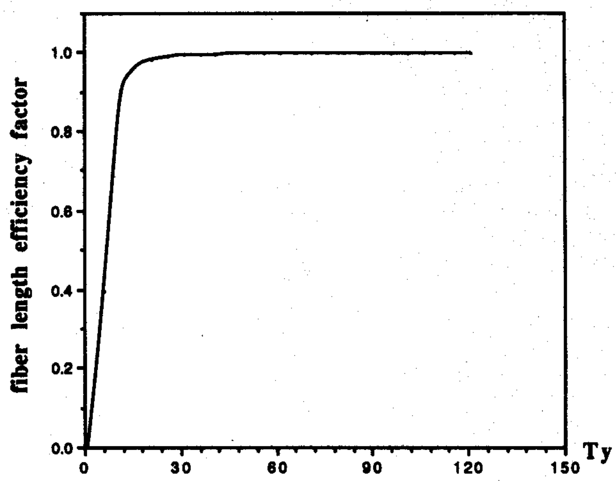

FIGURE 12. The length efficiency factor η_l versus yarn twist T_y.

Figure 13 shows the result for the longitudinal tensile modulus of the yarn. It is well known that a staple yarn modulus increases as the yarn twist level goes up from zero to a certain point; it then decreases along with the further increase of T_y. This is still the case even for our hypothetical yarn model where fiber end slippage has been excluded. The curve shown in Figure 13 is in fact the result of three competing factors—the yarn fiber-volume fraction V_f, the length efficiency factor η_l, both of which increase monotonically along with yarn twist level, and the effect of fiber obliquity caused by twist, which reduces the yarn modulus. The effect of this fiber obliquity is also depicted separately in Figure 14.

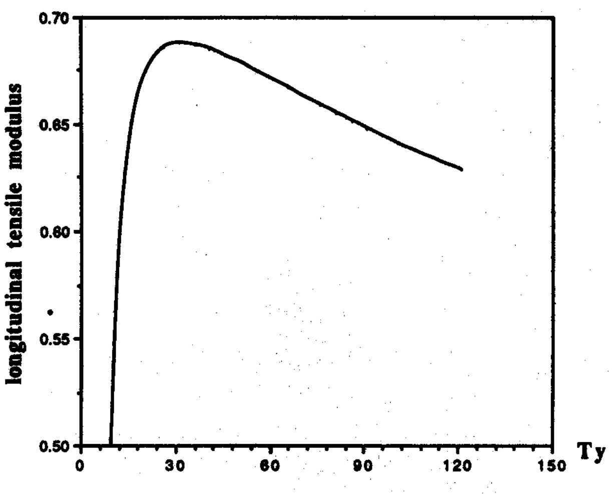

FIGURE 13. Relative yarn longitudinal tensile modulus E_L/E_f versus yarn twist T_y.

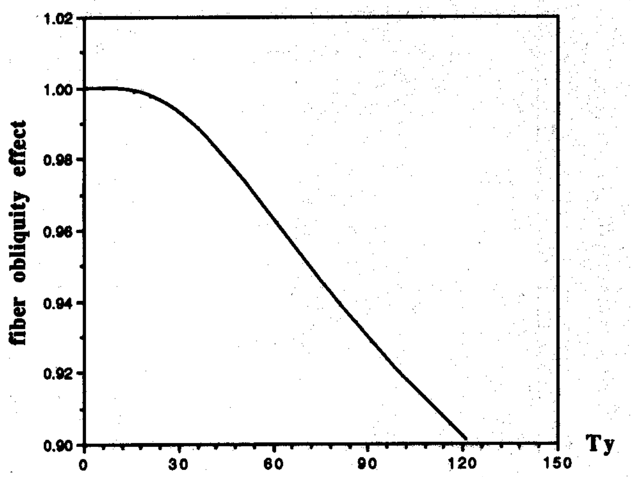

FIGURE 14. The effect of fiber obliquity versus yarn twist T_y.

We must admit that the fiber obliquity effect depicted in Figures 13 and 14 is not as significant as expected. The cause for this lies in the form of the fiber orientation density function used in the analysis, which specifies the fiber path in a yarn. Derivation of a more satisfactory density function will be the task in our subsequent paper, which will focus on the investigation of fiber orientation, including migration, in the yarn.

The result for the transverse tensile modulus of the yarn E_T is given in Figure 15. It indicates that initially E_T increases very rapidly as yarn twist goes up. It becomes stable once yarn twist is above a certain level.

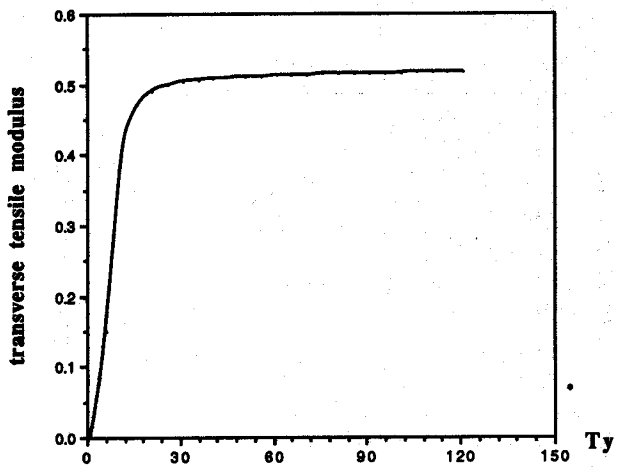

FIGURE 15. Relative yarn transverse tensile modulus E_T/E_f versus yarn twist T_y.

The relationships of both the longitudinal and transverse shear moduli of the yarn against the twist are shown in Figure 16. Both of them ascend monotonically but at significantly different rates with yarn twist. The whole structure thus grows tighter, making it more difficult for fibers to move relative to each other when more twist is inserted into the yarn. Both moduli approach the same level at the high twist region.

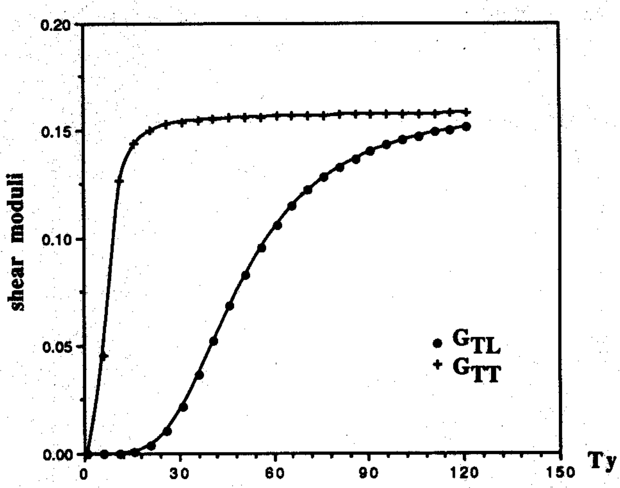

FIGURE 16. Relative yarn shear moduli G_{TL}/E_f and G_{TT}/E_f versus twist T_y.

It is interesting to see how the yarn Poisson's ratios change with twist level. When twist goes up, and yarn structure grows tighter, the Poisson's ratio ν_{LT}, governing induced transverse strains of the yarn due to longitudinal strain, decreases (see Figure 17), indicating that the effect of longitudinal strain on the trans-

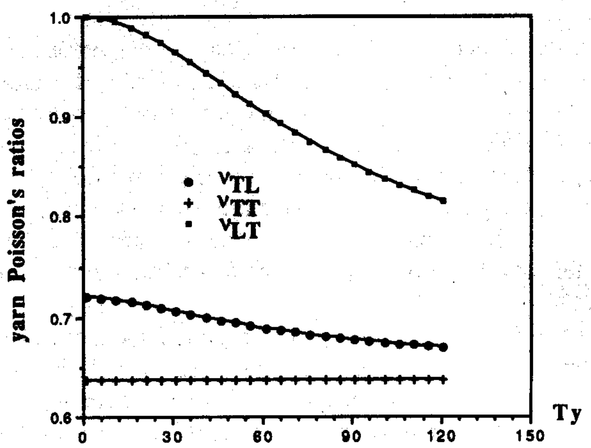

FIGURE 17. Poisson's ratios of yarn versus yarn twist T_y.

verse deformation becomes smaller. The Poisson's ratio ν_{TL}, governing induced longitudinal strains of the yarn due to transverse strain, shows a similar trend, meaning that transverse strain will also have a decreasing effect on longitudinal deformation of the yarn. The Poisson's ratio ν_{TT}, on the other hand, remains constant, showing that the interaction between the transverse strains is independent of the tightness of the structure.

Another point worth mentioning is that the values of these properties may appear too high. Note that a transversely isotropic material is different from an isotropic one whose Poisson's ratio is always less than 0.5. Jones [11] has reported $\nu_{LT} = 1.97$ for a boron-epoxy composite. In fact, the only restrictions on the permissible values of ν_{LT} and ν_{TL} are dictated in Equations 5 and 6, whereas the boundary of ν_{TT} for a transversely isotropic material [2] is $|\nu_{TT}| \leq 1$.

We have to stress, however, that the theory presented here does not consider fiber slippage, which will have a significant effect on yarn properties when yarn twist level is low. Therefore, the yarn mechanical behavior at the low twist levels shown above has to be modified. A modified theory including the fiber slippage effect will be introduced in the second part of this series.

Also, it is now possible to verify the constitutive restraints in Equations 5 and 6 on the tensile moduli and Poisson's ratios. The results are illustrated in Figures 18 and 19, showing clearly that both conditions are satisfied. This again confirms the validity of the analysis in this study.

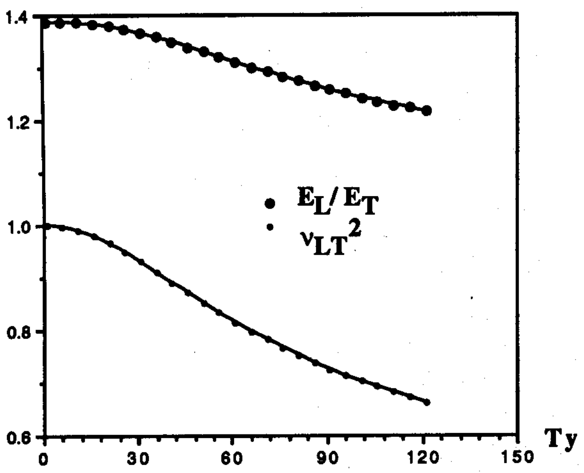

FIGURE 18. Verification of the constitutive restraint $\nu_{LT}^2 \leq \frac{E_L}{E_T}$.

Conclusions

We have developed a constitutive relationship for short fiber yarns without considering the effect of fiber end slippage. We have shown theoretically that, in general, both fiber tension and lateral pressure are not constant along a fiber length during yarn extension. The effectiveness of fiber gripping due to the frictional mechanism induced by yarn twist can be represented by the yarn cohesion factor defined in this study, which depends on yarn twist, fiber tensile modulus, and the form of fiber arrangement in the yarn.

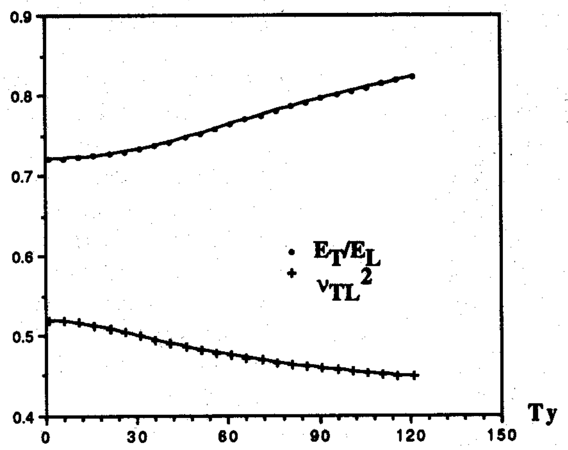

FIGURE 19. Verification of the constitutive restraint $\nu_{LT}^2 \leq \frac{E_T}{E_L}$.

Among the yarn mechanical properties derived in this study, the tensile and shear moduli are proportional to the fiber tensile modulus E_f, with the proportionality constants consisting of three parts, one being the fiber-volume fraction V_f, the second the length efficiency factor η_l in which the fiber dimensions are included, and the third reflecting the effect of fiber obliquity or fiber orientation distribution in the yarn. Twist alters the values of the yarn moduli through these factors. On the other hand, the yarn Poisson's ratios are related only to the fiber geometrical orientation within the yarn, and are independent of the fiber's intrinsic properties, if we ignore the effects of the fiber Poisson's ratios themselves.

ACKNOWLEDGMENT

My interest in yarn mechanics was initiated during my work in Professor Stanley Backer's research group at MIT. His help and encouragement have been of great value to me in pursuing this project. I would also like to acknowledge helpful discussions with Drs. B. C. Goswami, H. D. Wagner, and Y. J. Wang.

Appendix

NOMENCLATURE

X_1, X_2 and X_3 Cartesian coordinates

θ and ϕ — polar and the azimuthal angles of a fiber in a yarn

q — fiber helix angle at the yarn surface

$\Omega(\theta, \phi)$ — fiber orientation density function in the yarn

l_f and $L_f = l_f/2$ — fiber length and half-fiber length as used in the theoretical analysis

A_f — cross-sectional area of fibers

E_f and r_f — fiber tensile modulus and radius

μ_f and ρ_f — interfiber frictional coefficient and fiber specific density

V_f — fiber-volume fraction (the specific volume) of the yarn

A_{yj} — cross-sectional area of a yarn element in direction j

P_j — external load in direction j exerted on the yarn

C_j — external load in direction j exerted on an arbitrary fiber in the yarn

C_{jp} and C_{jn} — tangential and the normal components of C_j

n — cohesion factor reflecting the fiber gripping effectiveness of the yarn

η_l — fiber length efficiency factor reflecting the effect of finite fiber length

K_j — geometrical coefficient when an oriented fiber length l_f is projected to direction j

$M_{jk}{}^a$ — geometrical coefficients associated with the components of axial deformation caused by P_j in direction k

δ_{aj} — axial elongation of an arbitrary fiber in the yarn due to P_j

$\bar{\delta}_{jk}$ and $\bar{\delta}_{aj}$ — statistical mean deformation components in direction k due to P_j and the mean deformation component due to axial elongation of the yarn representative element

ϵ_{jj} and σ_{jj} — continuum tensile strain and stress of the yarn in direction j

γ_{jk} and τ_{jk} — continuum shear strain and stress of the yarn in direction j due to load P_k

E_{jj} — tensile elastic modulus of the yarn in direction j

G_{jk} — shear modulus of the yarn corresponding to shear stress τ_{jk}

ν_{jk} — Poisson's ratio of the yarn

E_T — transverse modulus governing uniaxial loading in the transverse (X_1 or X_2) direction of the yarn

E_L — longitudinal modulus governing uniaxial loading in the longitudinal (X_3) direction

G_{TL} — longitudinal shear modulus governing shear in the longitudinal direction

G_{TT} — transverse shear modulus governing shear in the transverse plane

ν_{TT} — associated Poisson's ratio governing resultant strains in the remaining orthogonal transverse (X_1 or X_2) direction of the yarn

ν_{TL} — associated Poisson's ratio governing induced longitudinal strains of the yarn

ν_{LT} — associated Poisson's ratio governing induced transverse strains of the yarn

Literature Cited

1. Backer, S., Tire Cord Structure and Properties, in "Mechanics of Pneumatic Tires," S. K. Clark, Ed., W.B.S. Monograph 122, U.S. Government Prints Office, Washington DC, 1970.
2. Christensen, R. M., "Mechanics of Composite Materials," John Wiley & Sons, New York, 1979, p. 79.
3. Cox, H. L., The Elasticity and Strength of Paper and Other Fibrous Materials, *Br. J. Appl. Phys.* **3,** 72 (1952).
4. Dogu, I., The Distribution of Transverse Pressure in a Twisted Yarn Allowing for the Fiber Migration and Variation of Fiber Packing Density, *Textile Res. J.* **42,** 726 (1972).
5. Goswami, B. C., Martindale, J. G., and Scardino, F. L., "Textile Yarns: Technology, Structure, and Applications," John Wiley & Sons, New York, 1977, p. 183.
6. Goswami, B. C., Fiber-Yarn Forecasting Research Direction, Proc. Engineered Fiber Selection Miniconference, Cotton Incorporated, Raleigh, November, 1988, p. 105.
7. Grosberg, P., and Smith, P. A., The Strength of Slivers of Relatively Low Twist, *J. Textile Inst.* **57,** 15 (1966).
8. Hamburger, W. J., The Industry Application of the Stress-Strain Relationship, *J. Textile Inst.* **40,** 700 (1949).
9. Hickie, T. S., and Chaikin, M., Some Aspects of Worsted-Yarn Structure, Part II: The Fiber-Packing Density in the Cross-Section of Some Worsted Yarns, *J. Textile Inst.* **65,** 433 (1974).
10. Hearle, J. W. S., Grosberg, P., and Backer, S., "Structural Mechanics of Yarns and Fabrics," vol. 1, Wiley-Interscience, New York, 1969, p. 180.
11. Jones, R. M., Stiffness of Orthotropic Materials and Laminated Fiber-Reinforced Composites, *AIAA J.* **12,** 112–114 (1974).
12. Kelly, A., and MacMillan, N. H., "Strong Solids," 3rd ed., Clarendon Press, Oxford, 1986, p. 29.

13. Kilby, W. F., The Mechanical Properties of Twisted Continuous-Filament Yarns, *J. Textile Inst.* **55**, T589 (1964).
14. Lee, D. H., Initial Compressional Behavior of Fiber Assembly (in Korean), Doctoral thesis, Seoul National University, 1985.
15. Lee, D. H., and Lee, J. K., Initial Compressional Behavior of Fiber Assembly, in "Objective Measurement: Applications to Product Design and Process Control," S. Kawabata, R. Postle, and M. Niwa, Eds., The Textile Machinery Society of Japan, Osaka, 1985, p. 613.
16. Pan, N., and Carnaby, G. A., Theory of the Shear Deformation of Fibrous Assemblies, *Textile Res. J.* **59**, 285 (1989).
17. Peirce, F. T., Tensile Tests for Cotton Yarns v. 'The Weakest Link' Theorems on the Strength of Long and of Composite Specimens, *J. Textile Inst.* **17**, 355 (1926).
18. Piggott, M. R., Load Bearing Fiber Composites, Pergamon Press, Oxford, 1980.
19. Platt, M. M., Mechanics of Elastic Performance of Textile Materials, Part III: Some Aspects of Stress Analysis of Textile Structures—Continuous Filament Yarns, *Textile Res. J.* **20**, 1 (1950).
20. Postle, R., Carnaby, G. A., and de Jong S., "The Mechanics of Wool Structure," Ellis Horwood Limited, England, 1988.
21. Riddle, E. R., Preliminary Considerations in a Plan of Work to Develop Fiber-Yarn Models, in "Proc. Engineered Fiber Selection Miniconference," Cotton Incorporated, Raleigh, November, 1988, p. 161.
22. Sullivan, R. R., A Theoretical Approach to the Problem of Yarn Strength, *J. Appl. Phys.* **13**, 157 (1942).
23. Treloar, L. R. G., Twisted Structures, *J. Textile Inst.* **55**, 13 (1964).
24. White, J. L., Chen, C. C., and Spruiell, J. E., Some Aspects of the Mechanics of Continuous Filament Twisted Yarns and the Deformation of Fibers, Applied Polymer Symposium, no. 27, p. 275, 1975.
25. Zurek, W., "The Structure of Yarn," 2nd ed., WNT, Warsaw, Poland, 1975.

Manuscript received April 21, 1992; accepted June 2, 1992.